Supplementary Information

Protein-responsive assemblies from catechol-metal ion supramolecular coordination

Conghui Yuan, Jiangfeng Chen, Shirong Yu, Ying Chang, Jie Mao, Yiting Xu, Weiang Luo, Birong Zeng, Lizong Dai*

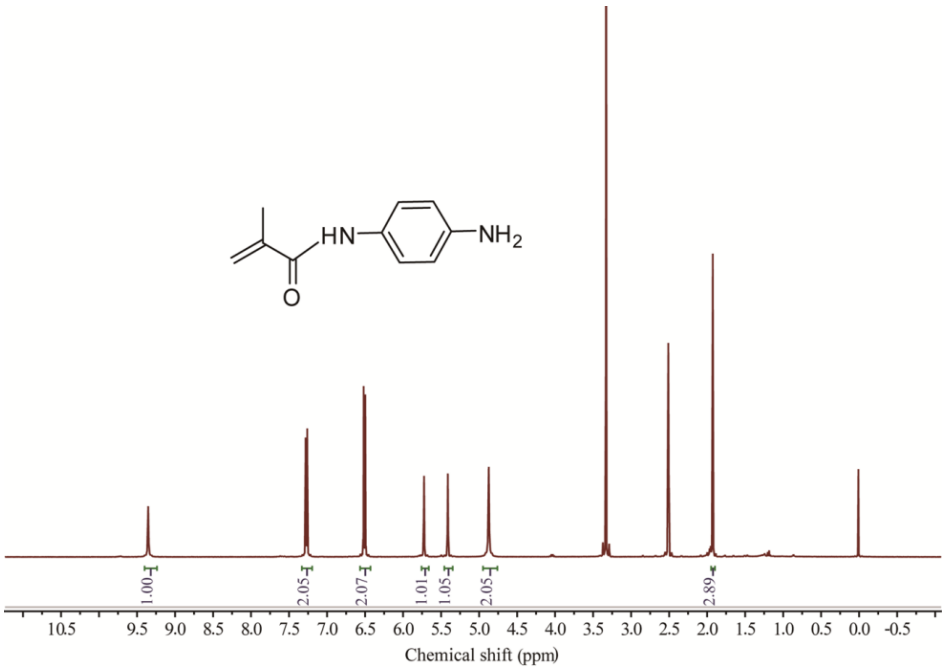

Figure S1. ^{1}H NMR spectrum of N-(4-aminophenyl)methacrylamide in DMSO-d6.

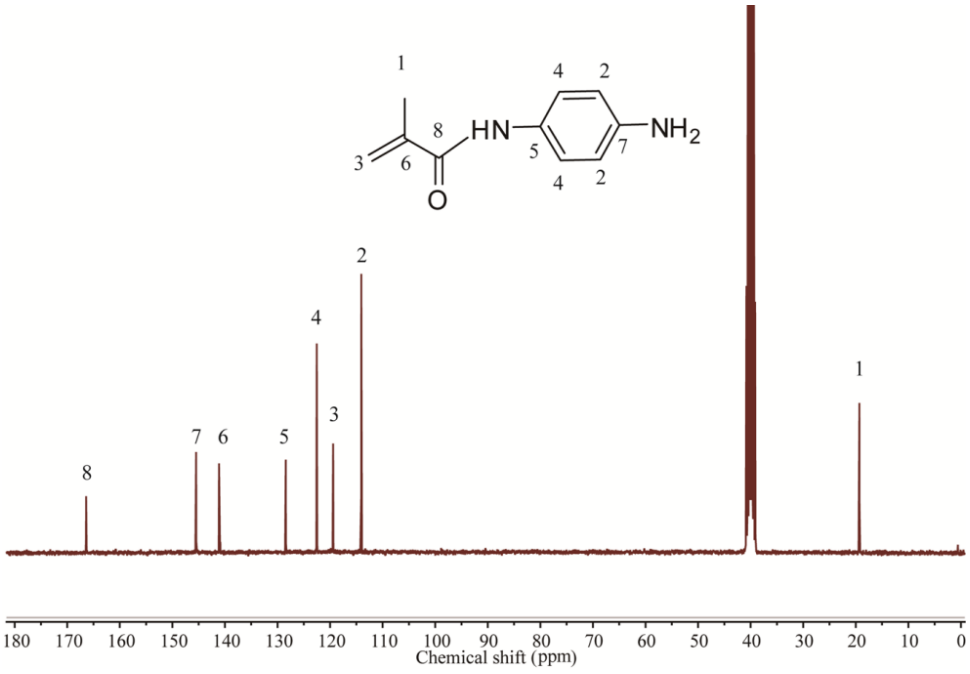

Figure S2. ^{13}C NMR spectrum of N-(4-aminophenyl)methacrylamide in DMSO-d6.

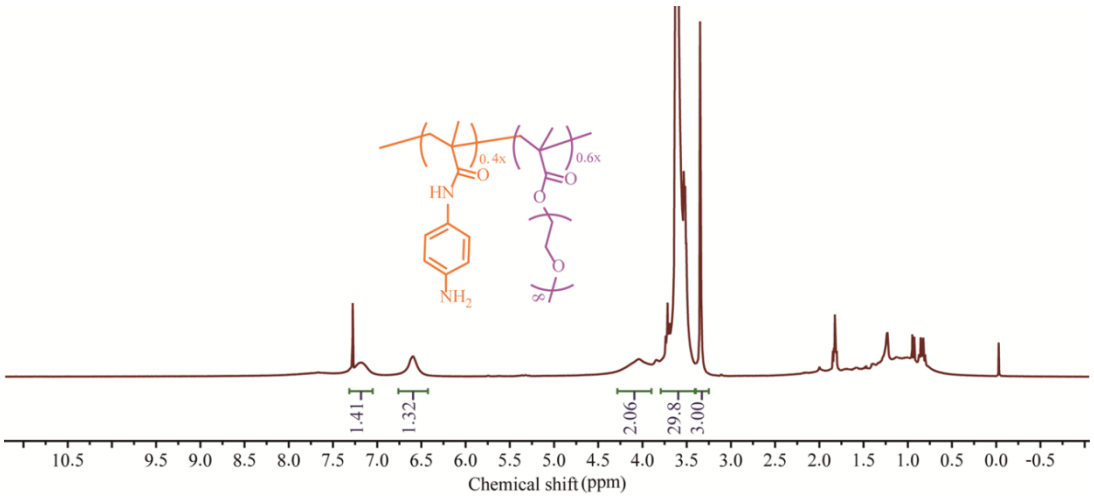

Figure S3. ^{1}H NMR spectrum of P(APMA-co-MAPEG) in $CDCl_3$.

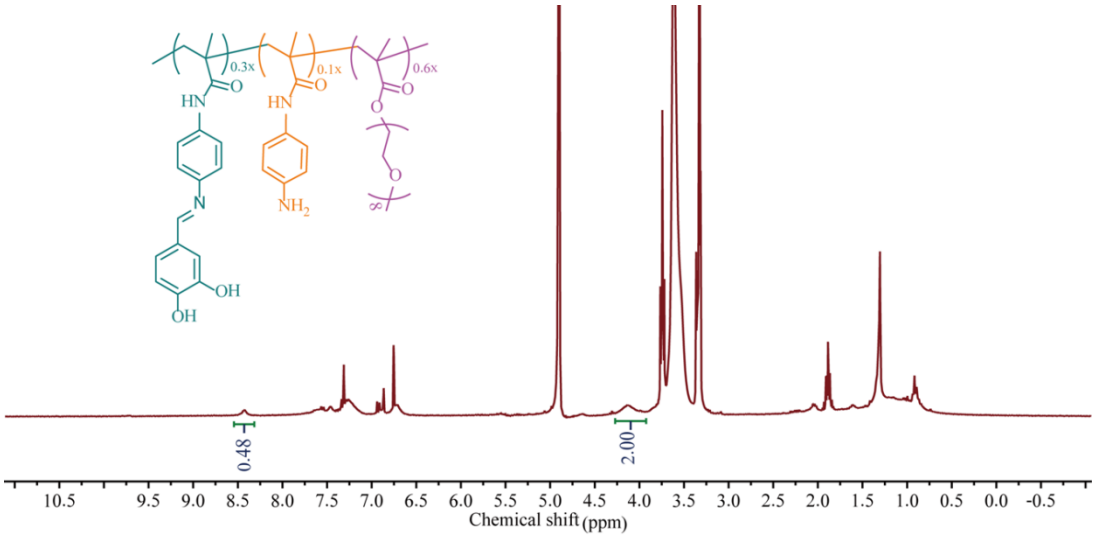

Figure S4. ^{1}H NMR spectrum of **CP** in methanol-d4.

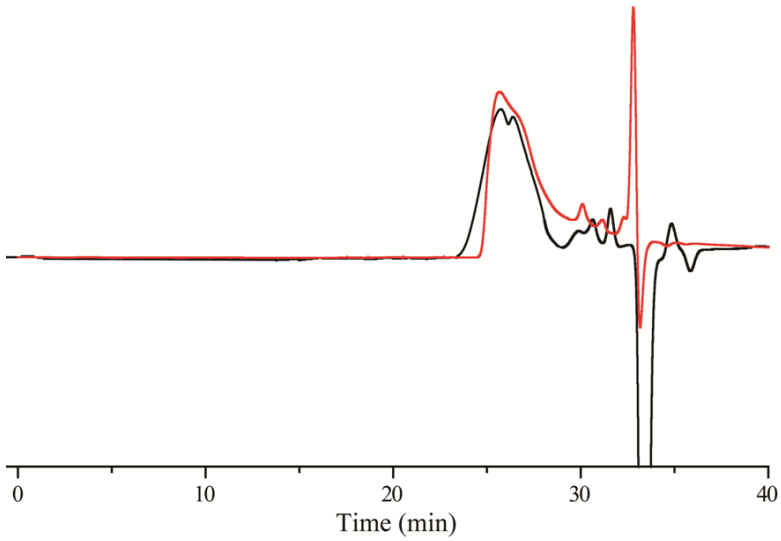

Figure S5. THF GPC curves of P(APMA-co-MAPEG) (red line) and **CP** (black line).

Table S1. Summary of M_n, M_w and Đ of P(APMA-co-MAPEG) and **CP**.

	M_n	M_w	Đ
P(APMA-co-MAPEG)	11806	17827	1.51
CP	12418	18376	1.48

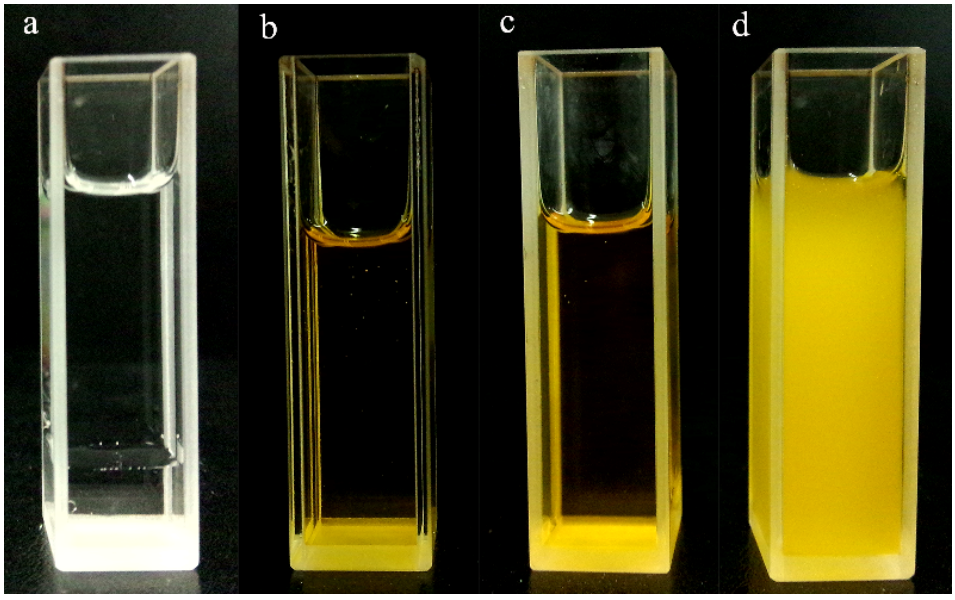

Figure S6. Photos of (a) the mixture of *n*-butanol (2.0 mL) and water (0.4 mL), (b) **CP**/water solution (10 mg/mL), (c) **CP**/*n*-butanol solution (10 mg/mL) and (d) the mixture containing 2.0 mL of *n*-butanol, 0.4 mL of water and 10 mg of **CP**.

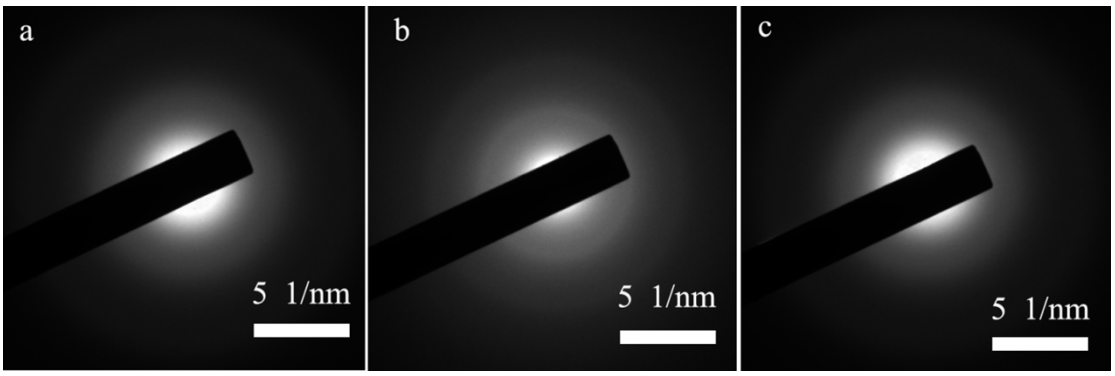

Figure S7. Electron diffraction patterns of **CP**-Fe^{3+} nanoassemblies derived from 1.0 (a), 2.0 (b) and 3.0 μmol/mL (c) of Fe^{3+}.

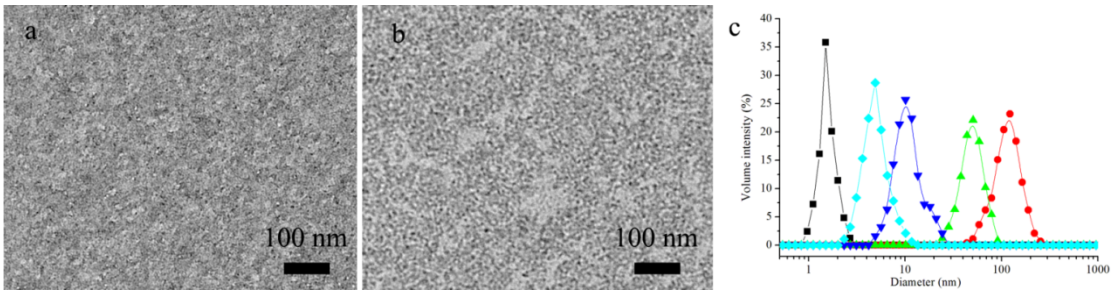

Figure S8. TEM images of **CP**-Fe^{3+} nanoassemblies formed by using 7.6 μmol/mL of Fe^{3+} (a) and the resultant **CP**-Fe^{3+} nanoassemblies after disassembly with the addition of 0.3 μmol/mL Fe^{3+} (b). DLS results tracking the disassembly of the **CP**-Fe^{3+} nanoassemblies with the addition of 0 (●), 0.1 (▲), 0.2 (▼) and 0.3 μmol/mL (◆) Fe^{3+}; (■) diameter of the **CP**-Fe^{3+} nanoassemblies formed by using 7.6 μmol/mL of Fe^{3+}. The **CP**-Fe^{3+} nanoassemblies used for this disassembly test were prepared by injecting 5.0 mL of **CP**/water solutions (~38.0 μmol catechol) with 10.0 mL of $FeCl_3 \cdot 6H_2O$/*n*-butanol solution (3.0 μmol/mL).

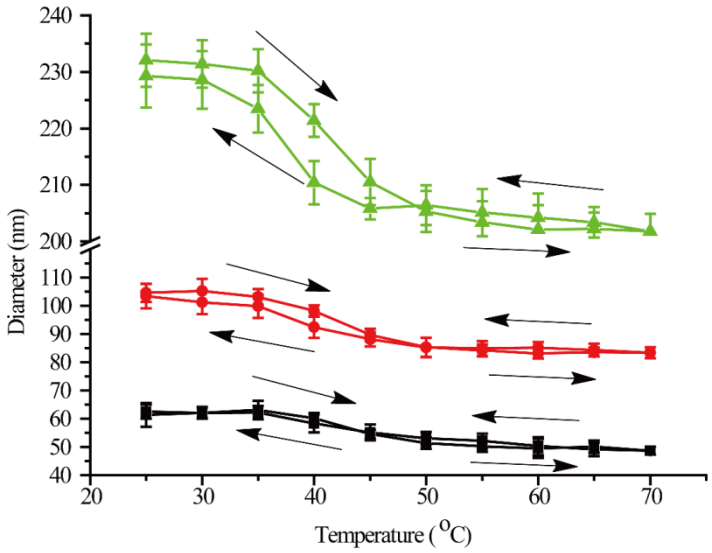

Figure S9. Diameter evolution of **CP**-Fe^{3+} assemblies under thermal-cycling. The as-used samples were: solid assemblies formed by injecting 5.0 mL of **CP**/water solution (~38.0 μmol catechol) into 10.0 mL of $FeCl_3 \cdot 6H_2O$/*n*-butanol solution with concentrations (■) 1.0 and (●) 2.0 μmol/mL, and (▲) vesicles prepared by injecting 6.0 mL of $FeCl_3 \cdot 6H_2O$/water solutions (containing 20 μmol of Fe^{3+}) into 10 mL of **CP**/*n*-butanol solution (5 mg/mL, ~38.0 μmol catechol group).

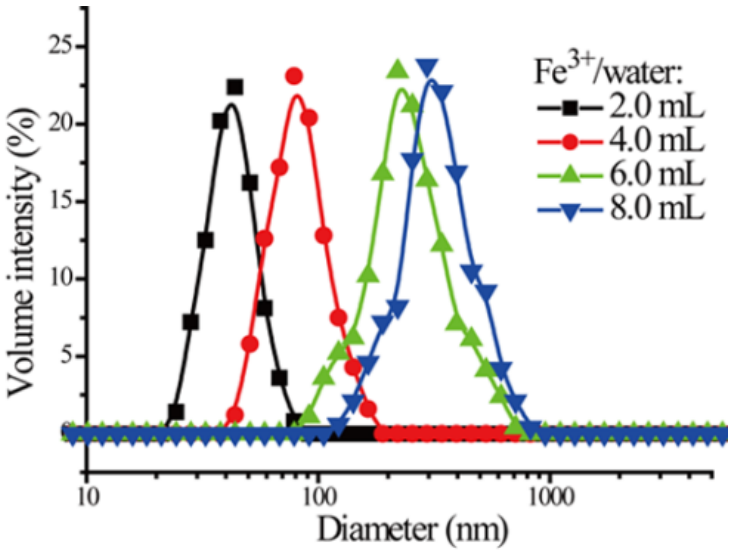

Figure S10. Diameter of **CP**-Fe^{3+} assemblies prepared by injecting (■) 2.0, (●) 4.0, (▲) 6.0 and (▼) 8.0 mL of $FeCl_3 \cdot 6H_2O$/water solutions (containing 20 μmol of Fe^{3+}) into 10 mL of **CP**/*n*-butanol solution (5 mg/mL, ~38.0 μmol catechol group). The PDI of these DLS results are 0.08, 0.09, 0.18 and 0.22, respectively.

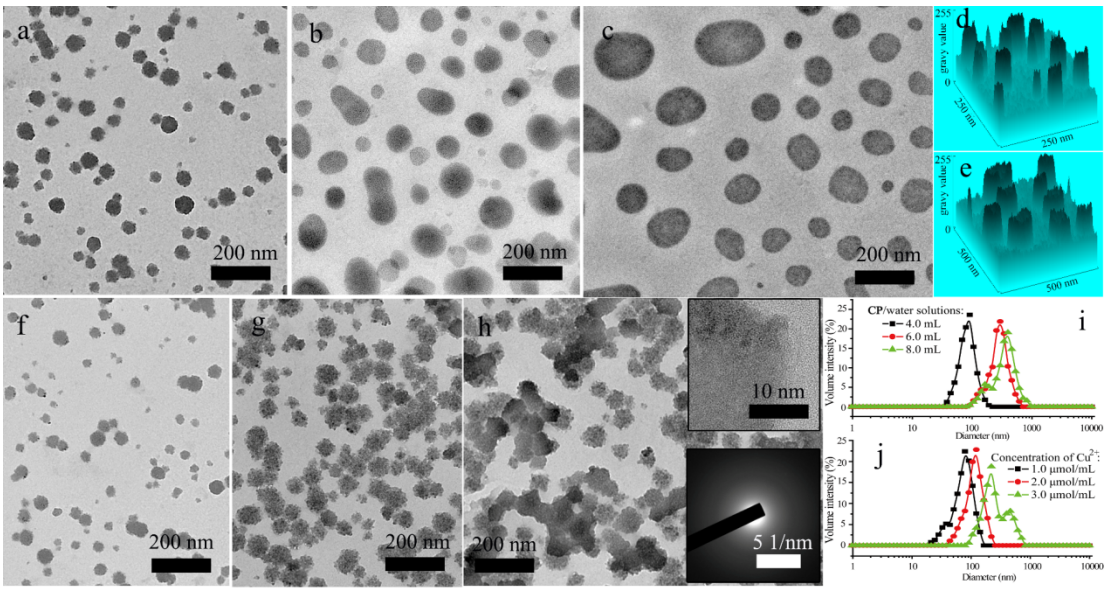

Figure S11. TEM images of **CP**-Cu^{2+} assembles prepared by injecting (a) 4.0, (b) 6.0 and (c) 8.0 mL of $CuCl_2 \cdot 2H_2O$/water solutions (20 μmol of Cu^{2+}) into 10 mL of **CP**/*n*-butanol solution (~38.0 μmol catechol). (d), (e) Gray value depended surface-imaging of TEM images (a) and (c). TEM images of **CP**-Cu^{2+} assembles formed by injecting 5.0 mL of **CP**/water solutions (~38.0 μmol catechol) into 10.0 mL of $CuCl_2 \cdot 2H_2O$/*n*-butanol solution with concentrations ranging from (f) 1, (g) 2.0 to (h) 3.0 μmol/mL. The top-right and bottom-right insets of (h) are the high resolution TEM image and electron diffraction pattern of the nanoassemblies, respectively. (i), (j) Diameters of the assemblies in water solution.

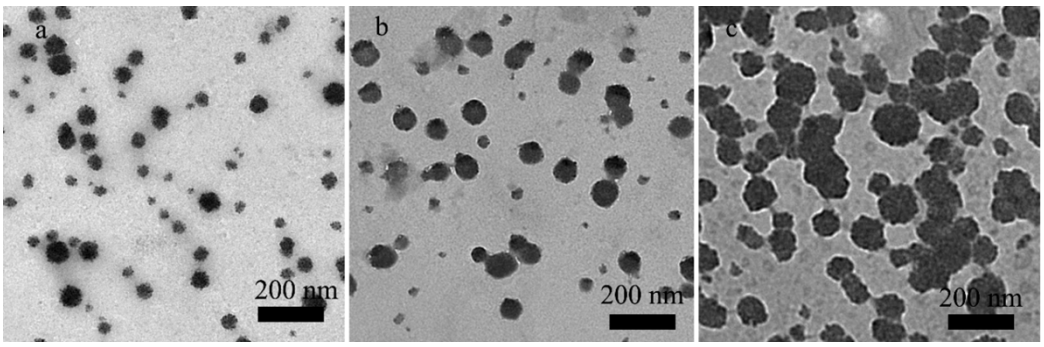

Figure S12. TEM images of **CP**-Cu^{2+} nanoassemblies formed by injecting 2.0 (a), 4.0 (b) and 6.0 mL (c) of **CP**/water solutions (~38.0 μmol catechol) into 10.0 mL $CuCl_2 \cdot 2H_2O$/*n*-butanol solution (2.0 μmol/mL). These nanoassemblies are solid and the diameter increased with the increasing volume of **CP**/water solution.

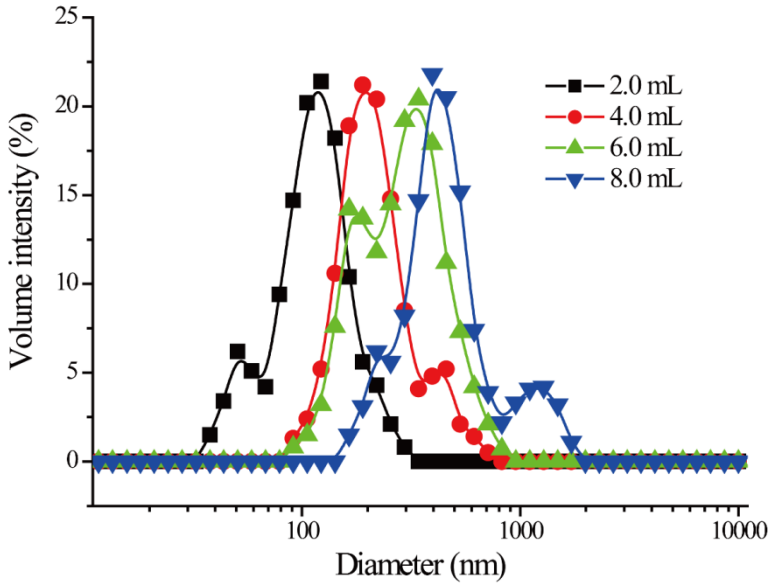

Figure S13. Diameter of emulsions formed by adding water with different volumes into 10 mL of **CP**/*n*-butanol solutions (10 mg/mL).

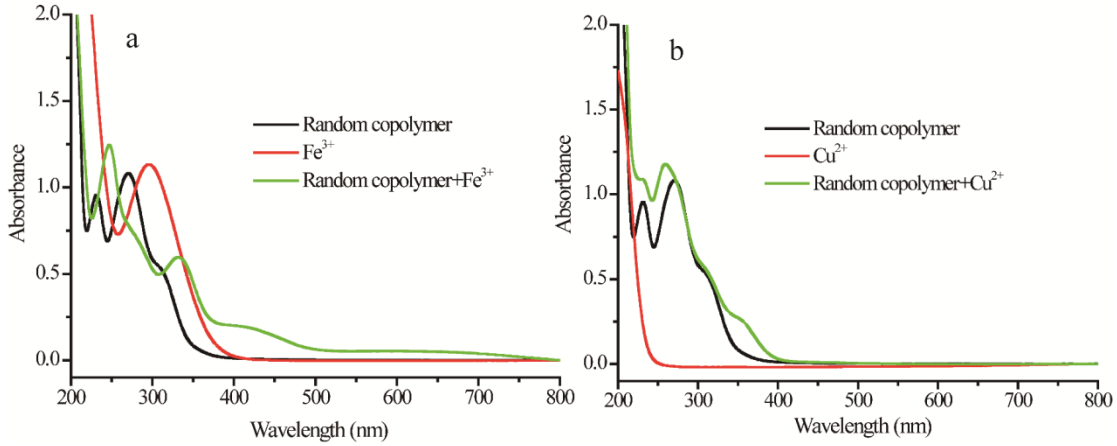

Figure S14. UV/vis spectra of $FeCl_3 \cdot 6H_2O$, $CuCl_2 \cdot 2H_2O$, **CP**, **CP**-Fe^{3+} nanoassemblies and **CP**-Cu^{2+} nanoassemblies in water solutions.

CP-Fe^{3+} nanoassemblies showed evident absorptions at 248 and 335 nm, **CP**-Cu^{2+} exhibited a characteristic absorption peak at 259 nm, which were different from the characteristic absorptions of **CP** (230 and 269 nm), Fe^{3+} (296 nm) and Cu^{2+} (lower than 200 nm).

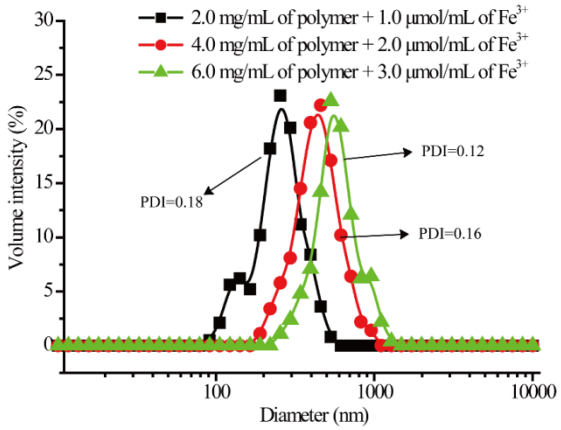

Figure S15. Particle sizes of the Janus vesicles formed by using different concentrations of both **CP** and $FeCl_3 \cdot 6H_2O$. These results were tested after transferring the Janus vesicles into the water solution.

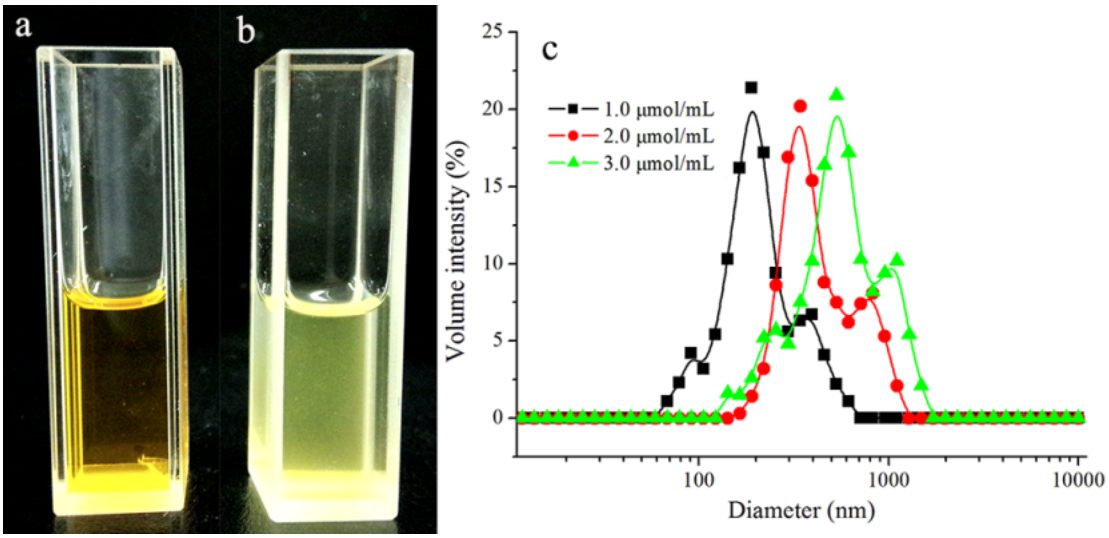

Figure S16. Photos of (a) $FeCl_3 \cdot 6H_2O$/*n*-butanol and (b) $FeCl_3 \cdot 6H_2O$/hexane solutions. (c) Diameter of $FeCl_3 \cdot 6H_2O$/hexane solutions with different concentrations.

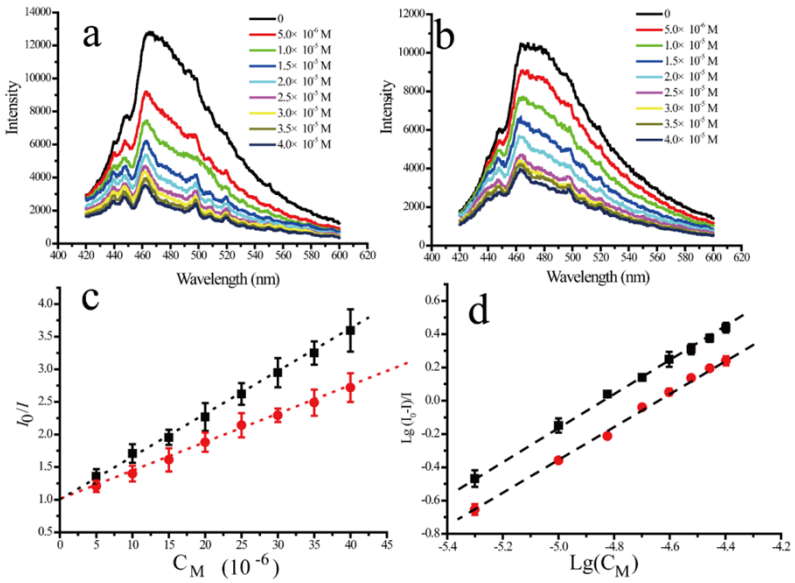

Figure S17. Fluorescence quenching of **CP** in water solution (pH=7.4) with the addition of (a) Fe^{3+} and (b) Cu^{2+}. The excitation wavelength and the maximum emission wavelength of this polymer were tested to be ~408 and ~463.5 nm, respectively. (c) Stern-Volmer curves of fluorescence quenching of **CP** with (■) Fe^{3+}, (●) Cu^{2+} calculated according to equation (1). (d) Double-logarithm plots of fluorescence quenching of **CP** with (■) Fe^{3+}, (●) Cu^{2+} calculated according to equation (2).

$$\frac{I_0}{I} = 1 + K_{sv} \bullet C_M \qquad (1)$$

$$Lg(\frac{I_0 - I}{I}) = Lg(K_s) + nLg(C_M) \qquad (2)$$

Where I_0 and I is the fluorescence intensities of **CP** at 463.5 nm in the absence and presence of metal ions; K_{sv} represents the dynamic quenching constant; C_M is the concentration of metal ions; K_s is the apparent stability constant; n represents the number of binding sites.

Through Figure 25S, $Lg(K_s)$ for Fe^{3+} binding to **CP** is ~4.95 and $Lg(K_s)$ for Cu^{2+} binding to **CP** is ~4.83.

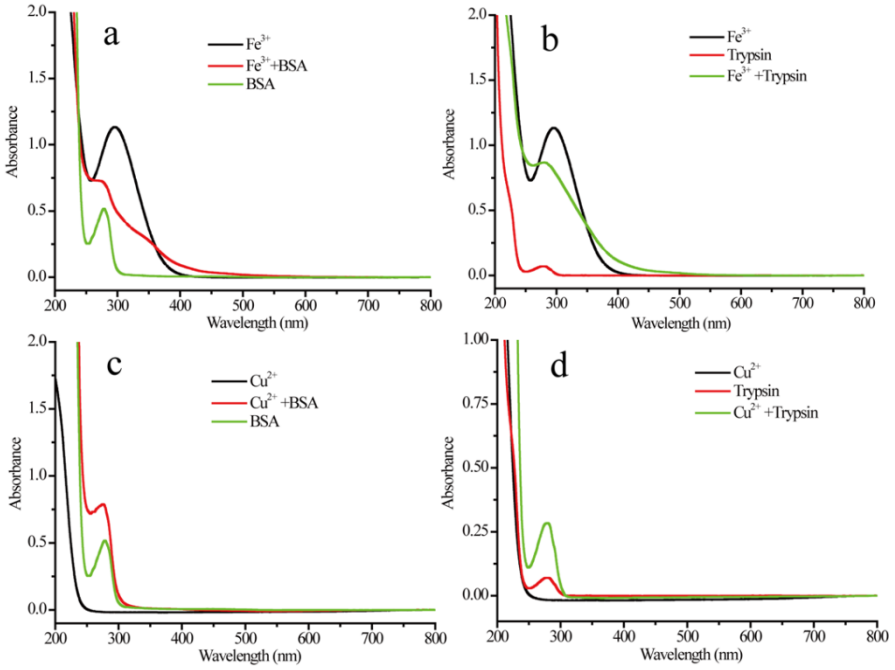

Figure S18. UV/vis spectra of $FeCl_3 \cdot 6H_2O$, $CuCl_2 \cdot 2H_2O$, BSA, trypsin and BSA-Fe^{3+}, trypsin-Fe^{3+}, BSA-Cu^{2+} and trypsin-Cu^{2+} complexes.

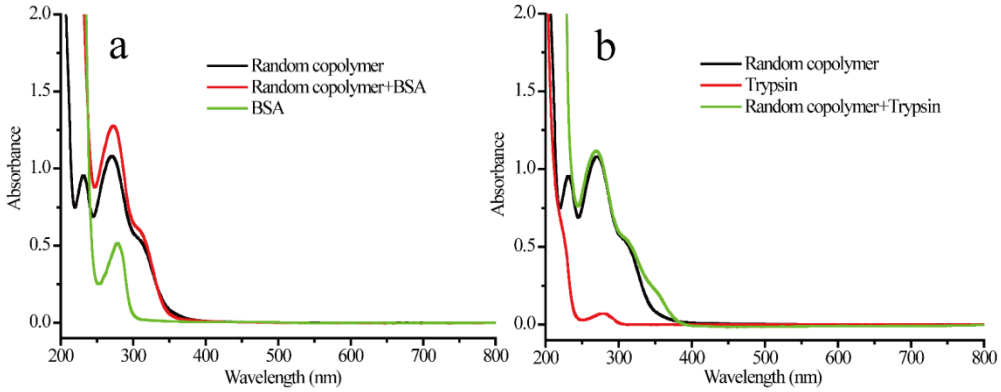

Figure S19. UV/vis spectra of BSA, trypsin, **CP**, **CP**+BSA and **CP**+trypsin.

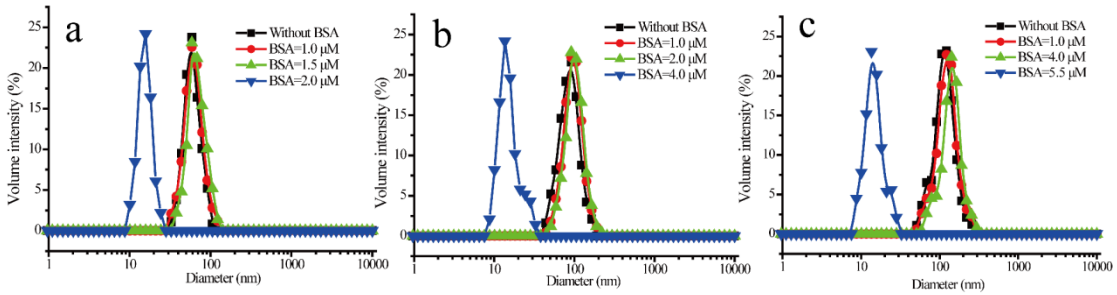

Figure S20. BSA triggered diameter evolution of **CP**-Fe^{3+} assemblies prepared by using $FeCl_3 \cdot 6H_2O$/*n*-butanol solutions with concentrations ranging from (a) 1.0, (b) 2.0 to (c) 3.0 μmol/mL (the morphology of the as-used assemblies were shown in Figure 1a-c).

Table S2. *CC* of the proteins for the disassembly of nanoassemblies: (a), (b) and (c) are the **CP**-Fe^{3+} assemblies prepared by using $FeCl_3 \cdot 6H_2O$/*n*-butanol solutions with concentrations ranging from 1.0, 2.0 to 3.0 μmol/mL; (d) **CP**-Fe^{3+} vesicles prepared from 6.0 mL of $FeCl_3 \cdot 6H_2O$/water solutions (20 μmol of Fe^{3+}) and 10 mL of **CP**/*n*-butanol solution (5 mg/mL, ~38.0 μmol catechol); (e) Janus vesicles derived from 4.0 mg/mL of **CP**/water solution and 2.0 μmol/mL of $FeCl_3 \cdot 6H_2O$/hexane solution.

CC	*a*	*b*	*c*	*d*	*e*
BSA	2.0 μM	4.0 μM	5.5 μM	3.5 μM	6.0 μM
Trypsin	2.5 μM	5.0 μM	6.0 μM	4.0 μM	7.0 μM

Table S3. *CC* of the proteins for the disassembly of nanoassemblies: (a), (b) and (c) are the **CP**-Cu^{2+} assemblies prepared by using $CuCl_2 \cdot 2H_2O$/*n*-butanol solutions with concentrations ranging from 1.0, 2.0 to 3.0 μmol/mL; (d) **CP**-Cu^{2+} vesicles prepared from 8.0 mL of $CuCl_2 \cdot 2H_2O$ /water solutions (20 μmol of Cu^{2+}) and 10 mL of polymer/*n*-butanol solution (5 mg/mL, ~38.0 μmol catechol).

CC	*a*	*b*	*c*	*d*
BSA	1.0 μM	1.5 μM	4.0 μM	1.0 μM
Trypsin	2.5 μM	3.5 μM	6.5 μM	3.0 μM

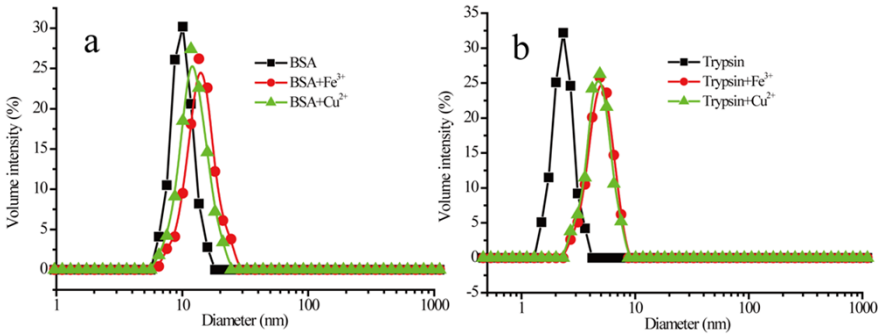

Figure S21. Diameters of BSA, Trypsin, BSA-Fe^{3+} complex, BSA-Cu^{2+} complex, Trypsin-Fe^{3+} complex and Trypsin-Cu^{2+} complex in aqueous solution.

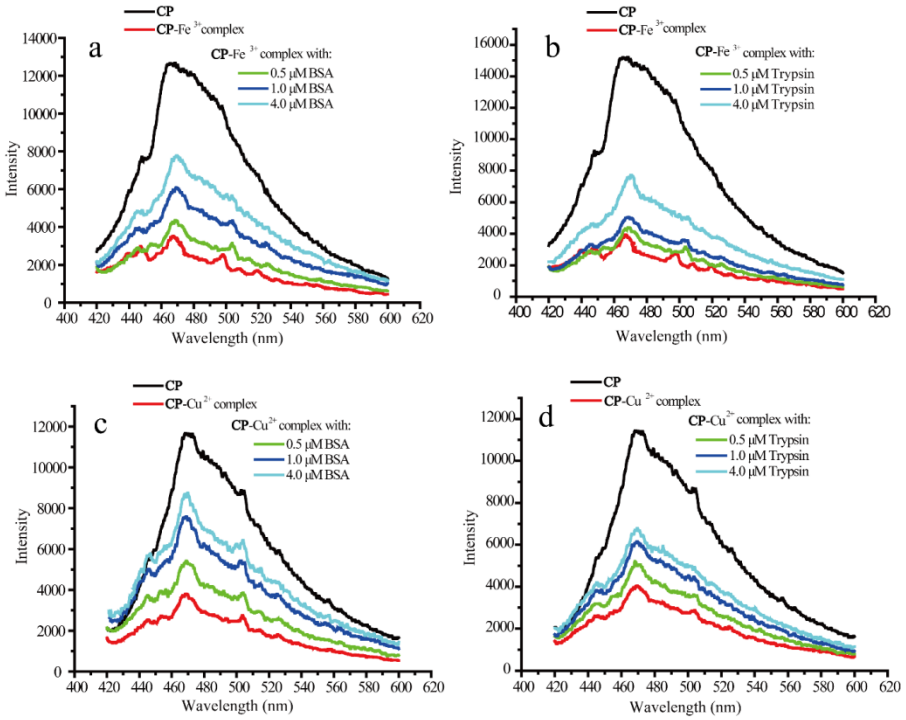

Figure S22. Fluorescence recovery of the **CP**-metal ion complexes triggered by proteins.

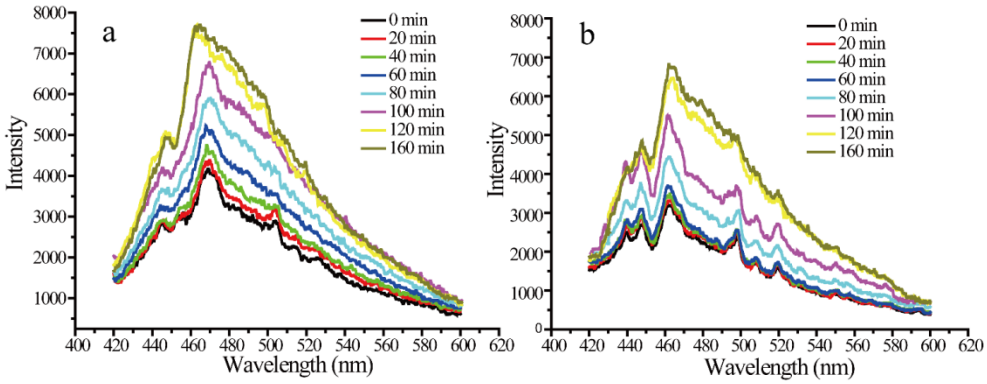

Figure S23. Fluorescence recovery kinetics of **CP**-Fe^{3+} complex triggered by BSA (a) and trypsin (b).